Appl. Comput. Harmon. Anal. ••• (••••) •••–•••

Contents lists available at ScienceDirect

Applied and Computational Harmonic Analysis

www.elsevier.com/locate/acha

Letter to the Editor

Reconstruction from circular and spherical mean data

Frank Filbir [a], Ralf Hielscher [a], W.R. Madych [b,*]

[a] Institute of Biomathematics and Biometry, HelmholtzZentrum München, Ingolstädter Landstraße 1, 85764 Neuherberg, Germany
[b] Department of Mathematics, 196 Auditorium Road, University of Connecticut, Storrs, CT 06269-3009, USA

ARTICLE INFO

Article history:
Communicated by Charles K. Chui on 19 September 2009

Keywords:
Image processing
Tomography

ABSTRACT

Circular and spherical mean data arise in various models of thermoacoustic and photoacoustic tomography which are rapidly developing modalities for *in vivo* imaging. We describe variants of a summability type reconstruction method adapted to this type of data. Among the highlights of the resulting algorithms, suggested by the results of numerical experiments, is the feature that the detectors need not lie on a regular curve or surface, such as a circle or a sphere. Several such numerical examples are included here.

1. Introduction

Given a sufficiently regular scalar valued function f on $\mathbb{R}^n$, $n \geqslant 2$, its spherical mean at ξ and r, where $\xi \in \mathbb{R}^n$ and $r > 0$, is the integral of f over the sphere of radius r centered at ξ. It can be expressed as the following integral over the unit sphere in $\mathbb{R}^n$

$$Sf(\xi, r) = \int_{\mathbb{S}^{n-1}} f(\xi + ru) r^{n-1} \, d\sigma(u) \tag{1}$$

where $d\sigma(u)$ denotes the usual surface measure on the unit sphere $\mathbb{S}^{n-1} = \{u \in \mathbb{R}^n : \ |u| = 1\}$. $Sf(\xi, r)$ is used to model the data in various models of thermoacoustic and photoacoustic tomography where f represents the phantom and ξ the position of a detector. More specifically, in such models the phantom f is taken to have compact support, usually in a ball, and the data $Sf(\xi, r)$ is known for ξ on the boundary of the supporting set, usually a sphere, and all relevant r.

The basic problem considered here is the following: Suppose $Sf(\xi, r)$ is known for ξ in a subset Ξ of R^n and all relevant r. Find an algorithm to reconstruct f.

Various aspects of this basic problem have been studied in great detail in the mathematical literature. The recent survey [4] contains a description of some of this work and a fairly exhaustive bibliography. See also the mathematically oriented articles in [8].

The objective of most of the mathematical literature is to obtain precise conditions for existence and uniqueness of solutions and, of course, exact reconstruction formulas and numerical procedures. The objective of the present article is to describe a heuristic procedure which gives rise to algorithms which provide good reconstructions under fairly general conditions. Thus by a reconstruction of f we mean an appropriate approximation of f.

Thermoacoustic and photoacoustic tomography are rapidly developing modalities for *in vivo* imaging. There are many technical articles on various engineering and biological aspects of the subject. For example, see [7], the recent collection [8],

* Corresponding author.
E-mail addresses: filbir@gsf.de (F. Filbir), ralf.hielscher@gsf.de (R. Hielscher), madych@math.uconn.edu (W.R. Madych).

1063-5203/$ – see front matter
doi:10.1016/j.acha.2009.10.001

Please cite this article in press as: F. Filbir et al., Reconstruction from circular and spherical mean data, Appl. Comput. Harmon. Anal. (2009), doi:10.1016/j.acha.2009.10.001

and the references cited there; [4] also contains a brief but informative discussion and many references to such material. Many of these articles contain a description of the relation between the measured data and spherical mean data; for example, the mathematically oriented article [1], among others found in [8], has such a description.

There are several equivalent definitions of the spherical mean $Sf(\xi, r)$ which differ only by a constant factor or a power of the variable r. The particular normalization used here is quite natural for certain practical applications and leads to a convenient formulation of our observations.

The general idea on which our reconstruction methodology is based is outlined in Section 2. The summability type reconstruction procedure is succinctly described in Section 3. Thus the impatient reader can skip directly to Section 3 for a straightforward description of the reconstruction method. Section 4 contains several specific numerical examples. We summarize our observations in Section 5.

2. Rationale

A function G on R^n is said to be *radial with center* ξ if there is a univariate function g such that $G(x) = g(|x - \xi|)$. If G is radial with center ξ then integrating its product with another function f on $\mathbb{R}^n$ and expressing the integral in terms of polar coordinates centered at ξ results in

$$\int_{\mathbb{R}^n} G(x) f(x)\, dx = \int_0^\infty \int_{\mathbb{S}^{n-1}} g(r) f(\xi + ru) r^{n-1} d\sigma(u)\, dr = \int_0^\infty g(r) Sf(\xi, r)\, dr. \tag{2}$$

We are of course assuming that all the functions involved are sufficiently well behaved so that the integrals make sense.

The rudimentary identity (2) is the basis of our method of reconstruction. Namely, if a function K can be expressed as a sum of functions that are respectively radial with centers ξ which are contained in a subset Ξ of $\mathbb{R}^n$ then the integral of the product of K and f can be computed from knowledge of the spherical means $Sf(\xi, r)$, $\xi \in \Xi$. Furthermore, if K is a good approximation of the identity at a point $x = x_0$ in R^n then the integral of the product will result in a good approximation of $f(x_0)$, thus giving rise to summability type reconstruction method. The definitions and formulas below are simply more precise versions of this observation.

Suppose Ξ is a measurable set and μ is a measure on Ξ. For instance, if Ξ is finite then a natural example of μ is the standard counting measure so that

$$\int_\Xi f(\xi)\, d\mu(\xi) = \sum_{\xi \in \Xi} f(\xi).$$

On the other hand, if Ξ is the unit sphere in R^n then a natural example would be the usual surface measure so that

$$\int_\Xi f(\xi)\, d\mu(\xi) = \int_{\mathbb{S}^{n-1}} f(u)\, d\sigma(u).$$

A locally integrable function K is a *sum of radial function with centers in* Ξ if there is a locally integrable function $k(\xi, r)$, $\xi \in \Xi$ and $r > 0$, and a measure μ on Ξ such that

$$K(x) = \int_\Xi k\big(\xi, |x - \xi|\big)\, d\mu(\xi). \tag{3}$$

If $K(x)$ enjoys representation (3) and $f(x)$ is an integrable function with compact support then in view of (2) we have

$$\int_{\mathbb{R}^n} K(x) f(x)\, dx = \int_\Xi \left\{ \int_0^\infty k(\xi, r) Sf(\xi, r)\, dr \right\} d\mu(\xi). \tag{4}$$

Hence, if the function K enjoys representation (3) and is a good approximation of the identity at some point $x = x_0$, i.e. $\int K(x) f(x)\, dx$ is a good approximation of $f(x_0)$ for sufficiently regular f, then formula (4) shows how to get a good approximation to $f(x_0)$ in terms of the spherical mean data $Sf(\xi, r)$, $\xi \in \Xi$ and $r > 0$.

In other words, if $\mathbf{K}(x, y)$, $(x, y) \in \mathbb{R}^n \times \mathbb{R}^n$, is a kernel that enjoys representation (3) in the y variable, i.e.

$$\mathbf{K}(x, y) = \int_\Xi k\big(x, \xi, |y - \xi|\big)\, d\mu(\xi), \tag{5}$$

then $\int \mathbf{K}(x, y) f(y)\, dy$ can be evaluated in terms of the spherical mean data $Sf(\xi, r)$, $\xi \in \Xi$ and $r > 0$. Specifically we have

$$\int_{\mathbb{R}^n} \mathbf{K}(x,y) f(y)\,dy = \int_{\Xi} \left\{ \int_0^{\infty} k(x,\xi,r) Sf(\xi,r)\,dr \right\} d\mu(\xi). \tag{6}$$

Now if f is sufficiently regular and has support in a region Ω and $\mathbf{K}(x,y)$ is a good approximation of the identity in y at each $x \in \Omega$ then identity (6) represents an approximate reconstruction of f in terms of the data $Sf(\xi,r)$, $\xi \in \Xi$ and $r > 0$. Such a kernel $\mathbf{K}(x,y)$ can be conveniently viewed as a family of functions in the y variable parameterized by x, each member of which is a sum of radial functions with centers in Ξ.

The natural assignment then is the following: Given the function K and the set Ξ find a solution k in representation (3).

Of course, not every pair K and Ξ will admit such a solution k. For example, if Ξ is a finite set with a small number of elements then it is unlikely that the set of functions K which admit representation (3) is sufficiently rich to include good approximations of the identity. On the other hand, if Ξ is a sphere, say $\Xi = \mathbb{S}^{n-1} = \{\xi \in R^n\colon\ |\xi| = 1\}$, then one might expect that the set of functions K which admit representation (3) is sufficiently rich to include good approximations of the identity, at least at points x inside the unit ball $B = \{x \in R^n\colon\ |x| < 1\}$.

The case when Ξ is a sphere is important. It is used as the model for many experimental setups [7,8] and has given rise to many important mathematical results [1,4]. However, unlike the analogous equation in the standard Radon transform model of tomography studied in [6], we are not aware of any reasonably simple solutions for k in terms of K.

We therefore take a heuristic approach.

Our objective is to find a family of radial functions $\{k(x,u,|x-u|)\}_{u\in\mathbb{S}^{n-1}}$ with centers on the unit sphere $\Xi = \mathbb{S}^{n-1} = \{u \in R^n\colon\ |u| = 1\}$ so that

$$\mathbf{K}(x,y) = \int_{\mathbb{S}^{n-1}} k\big(x,u,|y-u|\big)\,d\sigma(u) \tag{7}$$

is a good approximation of the identity in the variable y, $|y| < 1$, at least for points x close to the origin.

Look at the right-hand side of (7). We want the result to be a good point response function in the variable y at the point x where $|x| < 1$. Consider the solution h of

$$K(y) = \int_{\mathbb{S}^{n-1}} h\big(\langle y,u\rangle\big)\,d\sigma(u) \tag{8}$$

which is solvable whenever $K(y)$ is a reasonable radial function with center 0, see [6, Section 2]. If $K(y)$ is a good approximation of the identity at the origin then

$$K(x-y) = \int_{\mathbb{S}^{n-1}} h\big(\langle x,u\rangle - \langle y,u\rangle\big)\,d\sigma(u) \tag{9}$$

is a good approximation of the identity at x. For fixed u and x the function $h(\langle x,u\rangle - \langle y,u\rangle)$ is constant on $(n-1)$-dimensional hyperplanes (lines when $n=2$ or planes when $n=3$) perpendicular to u. On the other hand, the function $k(x,u,|y-u|)$ as a function of y is constant on spheres centered at u. Comparison of (7) and (9) and consideration of the respective geometrical setups suggest that the choice

$$k\big(x,u,|y-u|\big) = h\big(|x-u| - |y-u|\big)$$

might give rise to a reasonable approximation of the identity at the point x in the variable y, at least in cases when x is close to the center of the sphere and relatively far from the boundary.

The above choice for the function $k(x,u,|y-u|)$ can be further explained by the observation that

$$\lim_{r\to\infty} \big\{|x-ru| - |y-ru|\big\} = \langle y,u\rangle - \langle x,u\rangle \tag{10}$$

and the fact that h is even. Namely, if in (7) we replace $k(x,u,|y-u|)$ with $h(|x-ru| - |y-ru|)$ then in the limiting case as $r\to\infty$ the resulting identity reduces to (9).

With this rationale we consider kernels $\mathbf{K}(x,y)$ of the form

$$\mathbf{K}(x,y) = \int_{\mathbb{S}^{n-1}} h\big(|x-u| - |y-u|\big)\,d\sigma(u) \tag{11}$$

where h is a solution to (8) and the left-hand side of (8) is an approximation of the identity at the origin. Explicit formulas for such h can be found in [6, Section 3]. In Section 4 we consider specific examples and include results of numerical experiments in the practical cases $n=2$ and $n=3$, respectively. Some of these experiments seem to suggest that (11) gives rise to a good approximation of the identity even when the set of centers is not necessarily a sphere but a much more general collection of points.

Please cite this article in press as: F. Filbir et al., Reconstruction from circular and spherical mean data, Appl. Comput. Harmon. Anal. (2009), doi:10.1016/j.acha.2009.10.001

Reconstruction procedures based on analogies with the classical Radon transform are well known in photoacoustic and thermoacoustic imaging. For example, in [3] a variant of the so-called rho-filtered layergram method of classical tomography, a sum of backprojections followed by appropriate deconvolution, is considered. Backprojection methods based on regularization of existing inversion formulas are described in [2,5], see also Chapter 4 in [8] and related articles and citations found there. The procedure described here is, roughly speaking, a direct summability method analogous to that associated with the Fejer kernel and related kernels found in the theory of Fourier series. An application in classical tomography can be found, for example, in [6]. To our knowledge the summability type approximate reconstruction method described here is new and exact results are not yet known.

3. An approximate reconstruction procedure

Given spherical mean data, $Sf(\xi, r)$, $\xi \in \Xi$ and $r > 0$, we consider reconstructions or, more accurately, approximations $\tilde{f}$ of the phantom f in terms of this data which are of the form

$$\tilde{f}(x) = \int_{\Xi} \left\{ \int_0^{\infty} h\big(|x-\xi| - r\big) Sf(\xi, r)\, dr \right\} d\mu(\xi) \tag{12}$$

where $h(t)$ is a appropriately chosen function of one real variable t and $d\mu(\xi)$ is an appropriate measure on Ξ. More specifically, the function $h(t)$ is a solution to (8) and can also be expressed as

$$h(t) = K(0) + t \int_0^t \big(t^2 - s^2\big)^{-1/2} K'(su)\, ds \quad \text{when } n = 2 \tag{13}$$

and

$$h(t) = K(tu) + tK'(tu) \quad \text{when } n = 3, \tag{14}$$

where $K(x)$ is an radial function with center 0 chosen so that $K(x)$ is an approximation of the identity at the origin. Here u is any unit vector in $\mathbb{R}^2$ or $\mathbb{R}^3$ respectively and $K'(tu)$ denotes the derivative of $K(tu)$ with respect to the variable t. For these and other formulas relating $h(t)$ to $K(x)$ see [6, Section 2]. Specific examples of K and h in the cases $n = 2$ and 3 are given in Section 4.

4. Examples

The reconstructions below are considered in dimension two and three, i.e. $n = 2$ and $n = 3$, which are cases of practical interest.

The phantom $f(x)$ is taken to have support in the unit ball $B = \{x \in \mathbb{R}^n\colon\ |x| < 1\}$. Initially we take Ξ to be the unit sphere $\Xi = S^{n-1} = \{u \in R^n\colon\ |u| = 1\}$ (unit circle in the case $n = 2$) but subsequently consider much more general sets of detectors. Of course in the numerical calculations Ξ is taken to be a finite set and the sampling in the variable r is also discrete, say at $r = r_1, \ldots, r_m$ so that (12) reduces to

$$\tilde{f}(x) = c \sum_{\xi \in \Xi} \left\{ \sum_{i=1}^{m} h\big(|x-\xi| - r_i\big) Sf(\xi, r_i) \right\}, \tag{15}$$

where c is a conveniently chosen normalizing constant. For example,

$$1/c = a \sum_{y_j \in D} \sum_{\xi \in \Xi} h\big(|x-\xi| - |y_j - \xi|\big),$$

where D is the region of interest, y_j denotes the center of the jth pixel, and a is the pixel area.

4.1. Two-dimensional case

A convenient choice of $K(x)$ in Eqs. (13) is the so-called Poisson kernel

$$K_\epsilon(x) = \frac{1}{2\pi} \frac{\epsilon}{(\epsilon^2 + |x|^2)^{3/2}}.$$

The parameter $\epsilon > 0$ determines the thickness or resolution of K, the smaller the ϵ the better the resolution. The corresponding function $h(t)$ is

Please cite this article in press as: F. Filbir et al., Reconstruction from circular and spherical mean data, Appl. Comput. Harmon. Anal. (2009), doi:10.1016/j.acha.2009.10.001

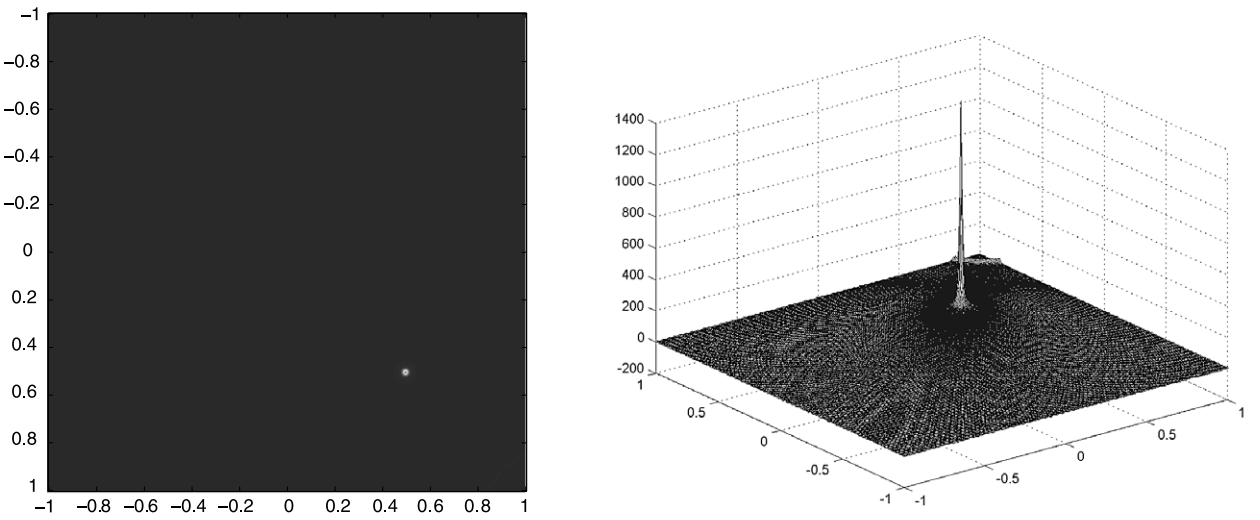

Fig. 1. $K_\epsilon(x, y)$ at $x = (0.5, 0.5)$, $|x| = 0.7071$.

$$h_\epsilon(t) = \frac{1}{2\pi}\frac{\epsilon^2 - t^2}{(\epsilon^2 + t^2)^2}. \tag{16}$$

See [6, (21)].

In the case that Ξ is the unit circle it is natural to parameterize it as $u_\theta = (\cos\theta, \sin\theta)$, $0 \leqslant \theta < 2\pi$, and discretize it by taking $\theta = \theta_1, \ldots, \theta_N$ where $\theta_j = 2\pi(j-1)/N$, $j = 1, \ldots, N$.

Figure 1. We exhibit the image and surface plot of

$$K_\epsilon(x, y) = \frac{1}{2\pi}\int_0^{2\pi} h_\epsilon\big(|x - u_\theta| - |y - u_\theta|\big)\, d\theta \tag{17}$$

as a function of y, $y \in [-1, 1] \times [-1, 1]$, for $x = (0.5, 0.5)$ so $|x| = 0.7071$. The function $h_\epsilon(t)$ is given by (16) with $\epsilon = 0.01$. This of course is equivalent to the phantom f being a point source (Dirac measure) at x in formula (12). As suggested by (15) formula (17) is numerically realized as

$$K_\epsilon(x, y) = c\sum_{j=1}^{N} h_\epsilon\big(|x - u_{\theta_j}| - |y - u_{\theta_j}|\big) \tag{18}$$

where $\theta_j = 2\pi(j-1)/N$, $j = 1, \ldots, N$, and c is a normalizing constant.

In the image and plot below $N = 300$ and the variable y ranges over a square grid of size 300×300.

For other points x in the unit disk $|x| < 1$, the images and plots of $K_\epsilon(x, y)$ as a function of y, $y \in [-1, 1] \times [-1, 1]$, are essentially indistinguishable from Fig. 1 *mutatis mutandis*.

Figure 2. We exhibit images of a phantom f, its data $Sf(u_{\theta_j}, r_i)$, $r_i = 2i/(M+1)$, $i = 1, \ldots, M$, $j = 1, \ldots, N$, and its reconstruction

$$\tilde{f}(x) = c\sum_{j=1}^{N}\left\{\sum_{i=1}^{M} h_\epsilon\big(|x - u_{\theta_j}| - r_i\big) Sf(u_{\theta_j}, r_i)\right\}$$

where $h_\epsilon(t)$ is given by (16) with $\epsilon = 0.01$. Thus the approximation of the identity is the one depicted in Fig. 1 with $x = (0.5, 0.5)$. As in Fig. 1, $N = 300$ and the independent variable, in this case x, ranges over a square grid of size 300×300. Furthermore, $M + 1 = 300$. The phantom f is a linear combination of indicator functions of ellipses and rectangles, the largest of which is a disk of radius 0.9.

Note that because the phantom is assumed to be supported in the unit disk, $|x| < 1$, and the detector sites ξ are on the unit circle, $|\xi| = 1$, the integrand in formula (12) vanishes for $r > 2$ so that the range of integration in the r variable is 0 to 2 in this example. In the numerically discrete case it reduces to the scenario mentioned above, namely, $r_i = 2i/(M+1)$, $i = 1, \ldots, M$. Specifically $\theta_j = 2\pi(j-1)/300$, $j = 1, \ldots, 300$, and $r_i = 2i/300$, $i = 1, \ldots, 299$.

Please cite this article in press as: F. Filbir et al., Reconstruction from circular and spherical mean data, Appl. Comput. Harmon. Anal. (2009), doi:10.1016/j.acha.2009.10.001

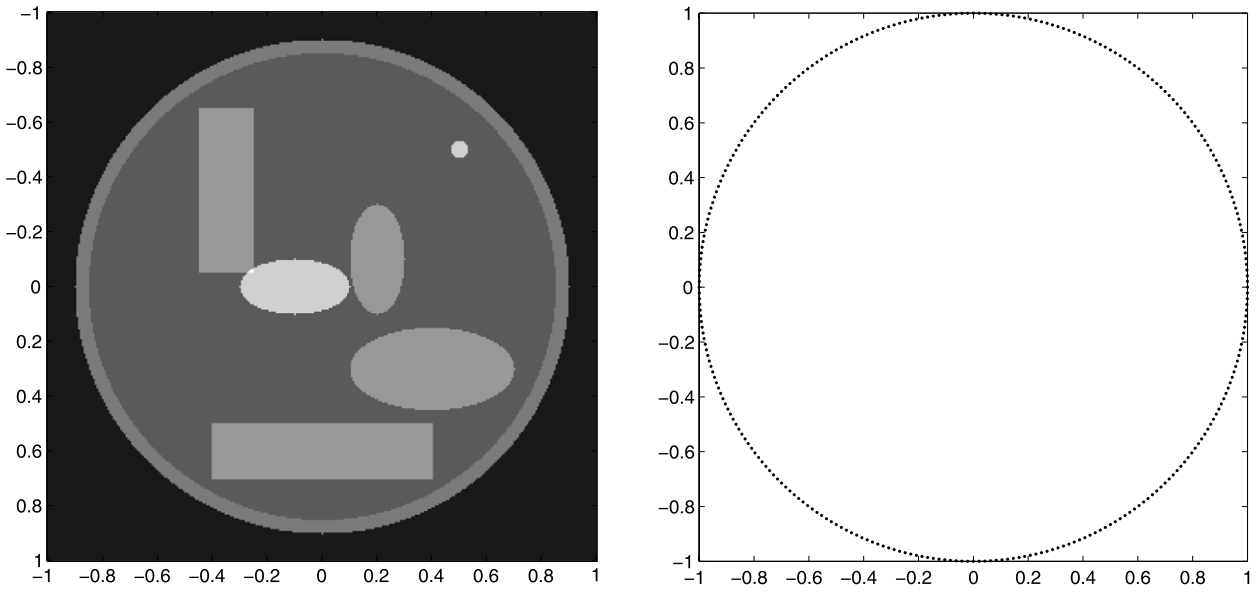

Fig. 2a. Phantom and detectors.

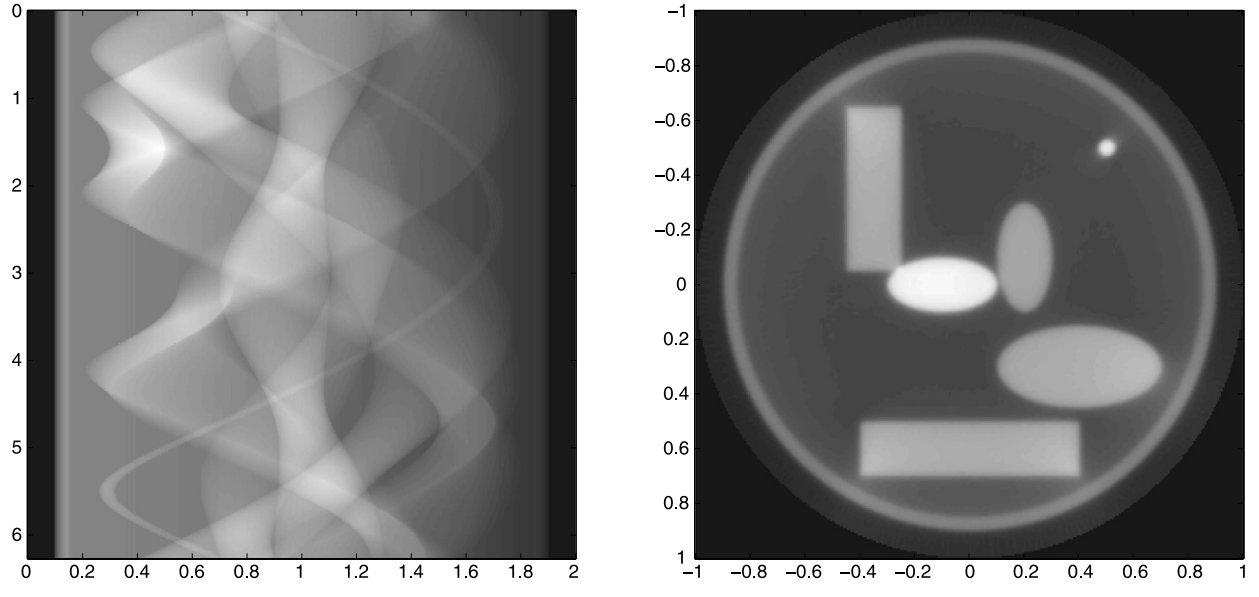

Fig. 2b. Data and reconstruction.

Figure 3. In this numerical experiment we use the same phantom as in Fig. 1 but take the detector sites ξ to be on the ellipse $(x/2)^2 + y^2 = 1$. In this case the variable ξ in formula (12) can be expressed as $\xi(\theta) = (2\cos\theta, \sin\theta)$, $0 \leqslant \theta < 2\pi$. Under the assumption that f has support in the unit disk for fixed θ the integrand will vanish outside the range $\rho(\theta) - 1 \leqslant r \leqslant \rho(\theta) + 1$, where $\rho(\theta) = \sqrt{(2\cos\theta)^2 + (\sin\theta)^2}$. So the discrete version of (12) becomes

$$\tilde{f}(x) = c \sum_{J=1}^{N} \left\{ \sum_{i=1}^{M} h_\epsilon\big(|x - \xi(\theta_j)| - r_i(\theta_j)\big) Sf\big(\xi(\theta_j), r_i(\theta_j)\big) \right\}.$$

We consider two types of data $Sf(u_{\theta_j}, r_i(\theta_j))$:

Data 1: $\theta_j = 2\pi(j-1)/300$, $j = 1, \ldots, 300$, and $r_i(\theta_j) = (\rho(\theta_j) + 1)i/300$, $i = 1, \ldots, 299$. In this case for each θ_j the sampling in the r variable is uniform over the interval $0 \leqslant r \leqslant \rho(\theta_j) + 1$. The size of the increment $r_{i+1}(\theta_j) - r_i(\theta_j) = (\rho(\theta_j) + 1)/300$ depends on θ_j so this should be taken into account when viewing the image of this data. Note that

Please cite this article in press as: F. Filbir et al., Reconstruction from circular and spherical mean data, Appl. Comput. Harmon. Anal. (2009), doi:10.1016/j.acha.2009.10.001

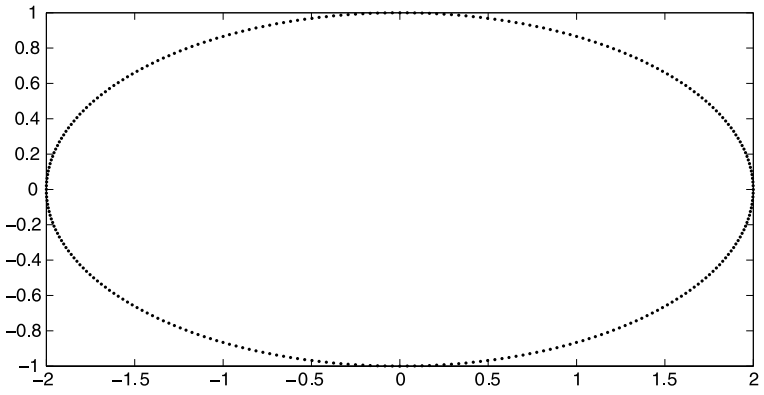

Fig. 3a. Detectors.

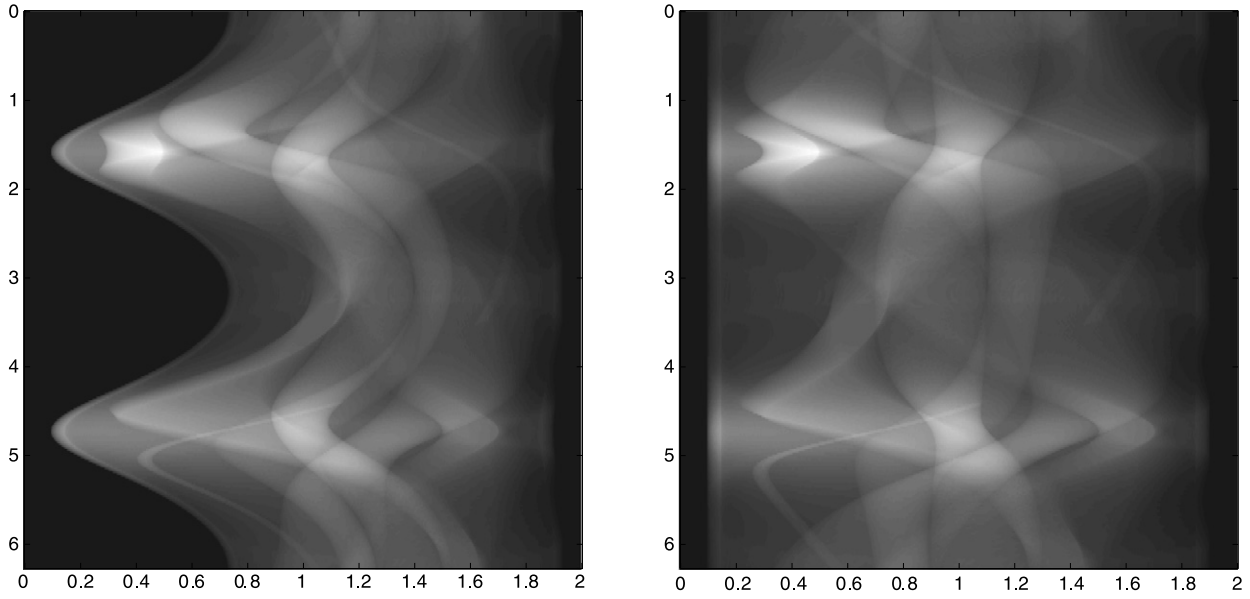

Fig. 3b. Data 1 and data 2.

$Sf(u_{\theta_j}, r_i(\theta_j)) = 0$ whenever $r_i(\theta_j) \leqslant \rho(\theta_j) - 1$ so that there is not as much effective data in this particular scheme as in Fig. 2.

Data 2: $\theta_j = 2\pi(j-1)/300$, $j = 1, \ldots, 300$, and $r_i(\theta_j) = (\rho(\theta_j) - 1) + 2i/300$, $i = 1, \ldots, 299$. In this case for each θ_j the sampling in the r variable is uniform over the interval $\rho(\theta_j) - 1 \leqslant r \leqslant \rho(\theta_j) + 1$, the total length of which is 2, and size of the increment $r_{i+1}(\theta_j) - r_i(\theta_j) = 2/300$ is independent of θ_j just as in the case of Fig. 2. This should be taken into account when viewing the image of this data. Apparently the amount of effective data in this particular scheme is the same as that in Fig. 2.

Figure 4. In this numerical experiment the of detectors ξ were somewhat randomly placed according to the following scheme:

$\xi(\theta_j) = (a_j \cos\theta_j, \sin\theta_j)$, $\theta_j = 2\pi(j-1)/300$, $j = 1, \ldots, 300$, and the coefficients a_j are independent pseudo random variables uniformly distributed on the interval $1 \leqslant a_j \leqslant 2$.

As in the case of Fig. 1 we present the corresponding image and plot of

$$K_\epsilon(x, y) = c \sum_{j=1}^{N} h_\epsilon\big(|x - \xi(\theta_j)| - |y - \xi(\theta_j)|\big)$$

as a function of y, $y \in [-1, 1] \times [-1, 1]$, for $x = (0.5, 0.5)$.

Please cite this article in press as: F. Filbir et al., Reconstruction from circular and spherical mean data, Appl. Comput. Harmon. Anal. (2009), doi:10.1016/j.acha.2009.10.001

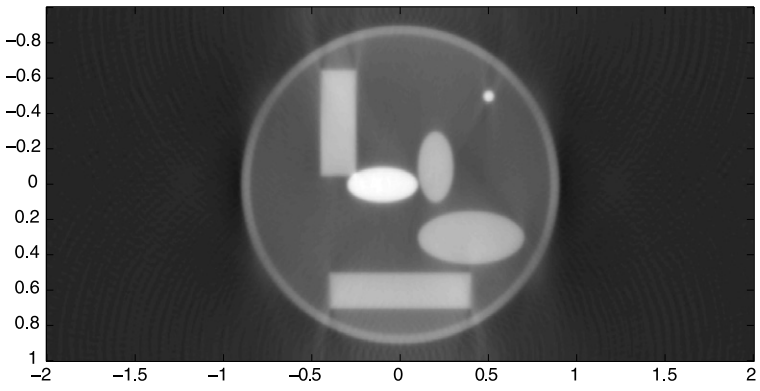

Fig. 3c. Reconstruction from data 1.

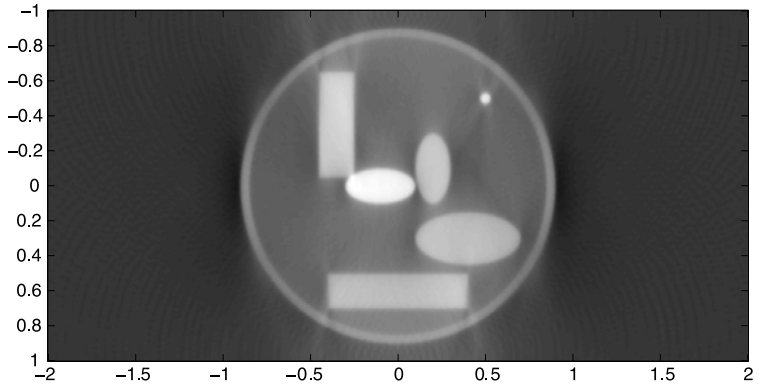

Fig. 3d. Reconstruction from data 2.

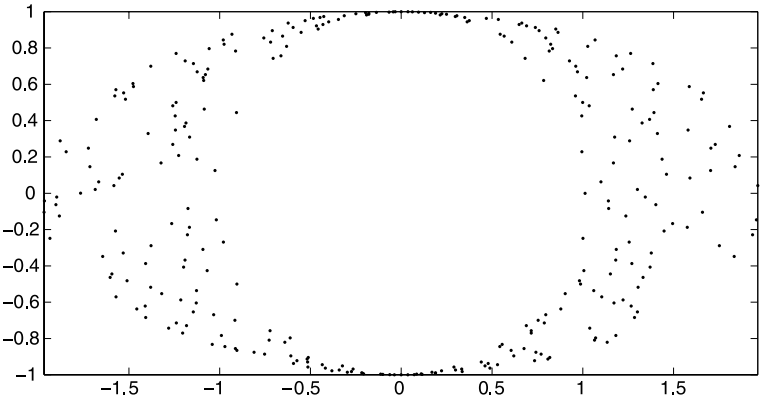

Fig. 4a. Detectors.

4.2. Three-dimensional case

In the three-dimensional case, i.e. $n = 3$, we consider the Gaussian kernel

$$K_\epsilon(x) = \frac{1}{(\epsilon\sqrt{\pi})^3} e^{-|x/\epsilon|^2}. \tag{19}$$

As in the case $n = 2$ the parameter $\epsilon > 0$ determines the thickness or resolution of K, the smaller the ϵ the better the resolution. The corresponding function $h(t)$ is

$$h_\epsilon(t) = \frac{1}{(\epsilon\sqrt{\pi})^3}\big(1 - 2(t/\epsilon)^2\big)e^{-|t/\epsilon|^2}. \tag{20}$$

Please cite this article in press as: F. Filbir et al., Reconstruction from circular and spherical mean data, Appl. Comput. Harmon. Anal. (2009), doi:10.1016/j.acha.2009.10.001

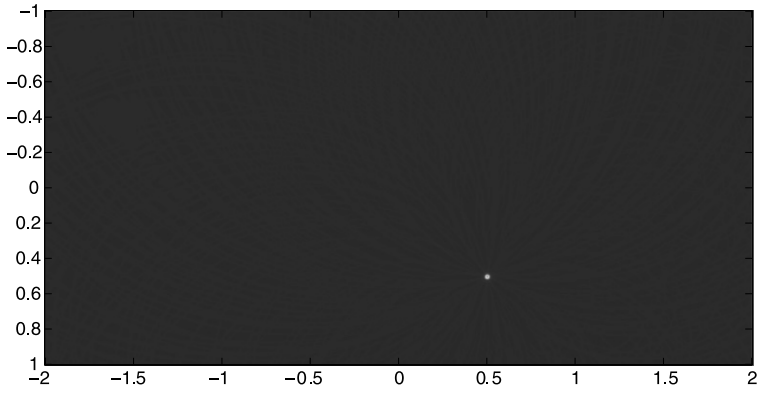

Fig. 4b. Image of $K_\epsilon(x, y)$, $x = (0.5, 0.5)$.

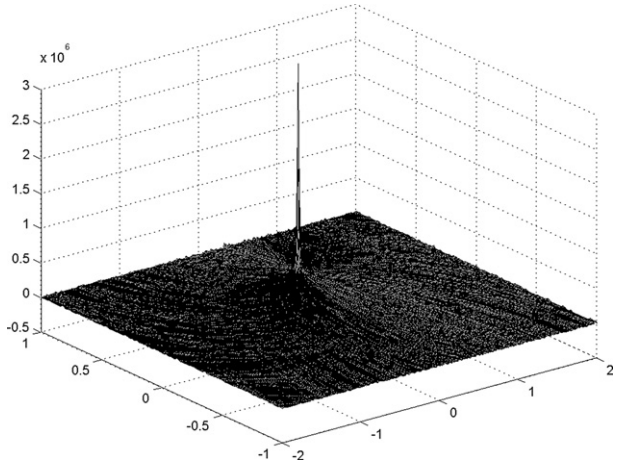

Fig. 4c. Plot of image in Fig. 4b.

In the case that Ξ is the unit sphere it is natural to parameterize it as $u_{(\theta,\phi)} = (\cos\theta \sin\phi, \sin\theta \sin\phi, \sin\phi)$, $0 \leqslant \theta < 2\pi$, $0 \leqslant \phi \leqslant \pi$, and discretize it by taking $\phi = \phi_0, \ldots, \phi_N$ where $\phi_j = j\pi/N$, $j = 0, \ldots, N$. The discretized parameter values θ should depend in some natural way on ϕ.

Figure 5. We exhibit the image of (19) and both the image and surface plots of

$$K_\epsilon(x, y) = c \sum_{j=0}^{N} \left\{ \sum_{m_j=0}^{M_j-1} h_\epsilon\big(|x - u_{(\theta_{m_j},\phi_j)}| - |y - u_{(\theta_{m_j},\phi_j)}|\big) \right\} \tag{21}$$

as a function of y, $y \in [-1, 1] \times [-1, 1] \times [-1, 1]$, for $\epsilon = 0.05$ and $x = (0.4, -0.4, 0.3)$ so $|x| = 0.6403$. The function $h_\epsilon(t)$ is given by (20). The other parameters are $\phi_j = \pi j/N$, $j = 0, 1, \ldots, N$, $M_j = \min\{4j, 4(N - j)\}$ and $\theta_{m_j} = 2\pi m_j/M_j$, $m_j = 0, \ldots, M_j - 1$. Specifically in the figure below $N = 32$ and the voxel size is 0.025, y takes on the values $y = (-1, -1, -1) + 0.025(i_1, i_2, i_3)$ where $i_j = 0, 1, \ldots, 80$ for $j = 1, 2, 3$.

The first row in the figure below contains the image of $K_\epsilon(x - y)$ as a function of $y = (y_1, y_2, y_3)$ followed by the image and surface plot of $K_\epsilon(x, y)$ as a function of $y = (y_1, y_2, y_3)$ in the plane $y_1 = 0.4$. The second and third rows contain the same sequence plotted in the planes $y_2 = -0.4$ and $y_3 = 0.3$, respectively.

5. Concluding remarks

To obtain reconstructions of the phantom f from its spherical mean data $Sf(\xi, r)$, $\xi \in \Xi$ and $r > 0$, it suffices to have good approximation of the identity kernels, or point response functions, $\mathbf{K}(x, y)$ of the form

$$\mathbf{K}(x, y) = \int_{\Xi} k\big(x, \xi, |y - \xi|\big)\, d\mu(\xi), \tag{22}$$

Please cite this article in press as: F. Filbir et al., Reconstruction from circular and spherical mean data, Appl. Comput. Harmon. Anal. (2009), doi:10.1016/j.acha.2009.10.001

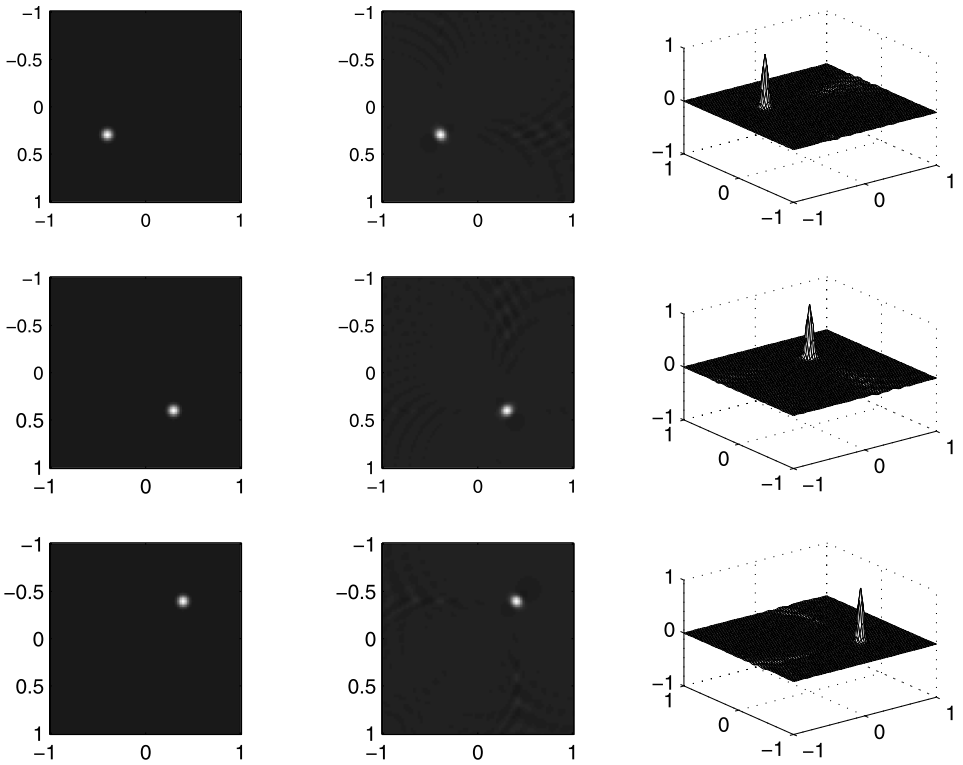

Fig. 5. The second and third columns contain the image and surface plots of (21) respectively restricted to the planes mentioned above.

because then $\int \mathbf{K}(x, y) f(y)\, dy$ can be computed in terms of the data. Our numerical experiments seem to indicate that by choosing

$$k\big(x, \xi, |y - \xi|\big) = h\big(|x - \xi| - |y - \xi|\big)$$

where $h(t)$, $-\infty < t < \infty$, is a solution of

$$K(y) = \int_{\mathbb{S}^{n-1}} h\big(\langle y, u\rangle\big)\, d\sigma(u)$$

with an appropriate radial function $K(y)$ can lead to good point response functions $\mathbf{K}(x, y)$ in (22) for various sets, spherical and otherwise, of detectors Ξ.

References

[1] D. Finch, Rakesh, Recovering a function from its spherical mean values in two and three dimensions, in: L. Wang (Ed.), Photoacoustic Imaging and Spectroscopy, CRC Press, 2009.
[2] D. Finch, M. Haltmeier, Rakesh, Inversion of spherical means and the wave equation in even dimensions, SIAM J. Appl. Math. 68 (2) (2007) 392–412.
[3] R.A. Kruger, P. Liu, Y.R. Fang, C.R. Appledorn, Photoacoustic ultrasound (PAUS) – reconstruction tomography, Med. Phys. 22 (10) (1995) 1605–1609.
[4] P. Kuchment, L. Kunyansky, Mathematics of thermoacoustic tomography, Eur. J. Appl. Math. 19 (02) (2008) 191–224.
[5] L.A. Kunyansky, Explicit inversion formulae for the spherical mean radon transform, Inverse Problems 23 (2007) 373–383.
[6] W.R. Madych, Summability and approximate reconstruction from radon transform data, Contemp. Math. 113 (1990) 189–219.
[7] D. Razansky, V. Ntziachristos, Hybrid photoacoustic florescence molecular tomography using finite-element-based inversion, Med. Phys. 34 (11) (Nov 2007) 4293–4301.
[8] L. Wang (Ed.), Photoacoustic Imaging and Spectroscopy, CRC Press, Boca Raton, 2009.

Please cite this article in press as: F. Filbir et al., Reconstruction from circular and spherical mean data, Appl. Comput. Harmon. Anal. (2009), doi:10.1016/j.acha.2009.10.001